



Two Dobzhansky-Muller Genes Interact to Cause Hybrid Lethality in *Drosophila*

Nicholas J. Brideau, *et al.*
Science **314**, 1292 (2006);
DOI: 10.1126/science.1133953

The following resources related to this article are available online at www.sciencemag.org (this information is current as of November 30, 2006):

Updated information and services, including high-resolution figures, can be found in the online version of this article at:

<http://www.sciencemag.org/cgi/content/full/314/5803/1292>

Supporting Online Material can be found at:

<http://www.sciencemag.org/cgi/content/full/314/5803/1292/DC1>

A list of selected additional articles on the Science Web sites **related to this article** can be found at:

<http://www.sciencemag.org/cgi/content/full/314/5803/1292#related-content>

This article **cites 21 articles**, 12 of which can be accessed for free:

<http://www.sciencemag.org/cgi/content/full/314/5803/1292#otherarticles>

This article appears in the following **subject collections**:

Evolution

<http://www.sciencemag.org/cgi/collection/evolution>

Information about obtaining **reprints** of this article or about obtaining **permission to reproduce this article** in whole or in part can be found at:

<http://www.sciencemag.org/help/about/permissions.dtl>

32. K. P. Burnham, D. R. Anderson, *Model Selection and Inference: A Practical Information-Theoretic Approach* (Springer, New York, ed. 2, 2002).
 33. R. Royall, *Statistical Evidence: A Likelihood Paradigm* (Chapman and Hall, London, 1997).
 34. T. D. Olszewski provided computer code to calculate zero-sum multinomials. R. Bambach, M. Foote, D. Jablonski,

S. K. Lyons, and J. McElwain provided critical comments. W. Kiessling and M. Kowalewski provided valuable reviews. P.J.W.'s contributions were funded in part by NSF grant EAR-0207874. This is PDBB publication #48.

Supporting Online Material
www.sciencemag.org/cgi/content/full/314/5803/1289/DC1

Materials and Methods
 Figs. S1 to S8
 Tables S1 to S3
 References

14 August 2006; accepted 2 October 2006
 10.1126/science.1133795

Two Dobzhansky-Muller Genes Interact to Cause Hybrid Lethality in *Drosophila*

Nicholas J. Brideau,* Heather A. Flores,* Jun Wang,* Shamoni Maheshwari, Xu Wang, Daniel A. Barbash†

The Dobzhansky-Muller model proposes that hybrid incompatibilities are caused by the interaction between genes that have functionally diverged in the respective hybridizing species. Here, we show that *Lethal hybrid rescue* (*Lhr*) has functionally diverged in *Drosophila simulans* and interacts with *Hybrid male rescue* (*Hmr*), which has functionally diverged in *D. melanogaster*, to cause lethality in F1 hybrid males. LHR localizes to heterochromatic regions of the genome and has diverged extensively in sequence between these species in a manner consistent with positive selection. Rapidly evolving heterochromatic DNA sequences may be driving the evolution of this incompatibility gene.

Plant and animal hybrids are often sterile or lethal as a result of interspecific genetic divergence. The Dobzhansky-Muller model proposes that hybrid incompatibilities (HIs),

which contribute to speciation, evolve as a consequence of interactions between or among genes that have diverged in each of the hybridizing species (1). Dobzhansky-Muller incompatibility

genes require three criteria: Each gene reduces hybrid fitness, has functionally diverged between the hybridizing species, and depends on the partner gene to cause HI (Fig. 1A). Major-effect HI genes have been discovered, and functional divergence of single genes has been demonstrated by genetic tests (2, 3) or suggested by patterns of molecular evolution (4). Although HI systems composed of complementary factors have been described (5, 6) and interacting genomic regions of hybridizing species identified (7–9), no pair of Dobzhansky-Muller genes has been reported. It remains unclear whether HI phenotypes can be explained even in part by two-locus interactions, or alternatively whether HIs require complex multilocus interactions (10–12).

Interspecific crosses of *D. melanogaster* females to *D. simulans* males produce no sons.

Department of Molecular Biology and Genetics, Cornell University, Ithaca, NY 14853, USA.

*These authors contributed equally to this work.

†To whom correspondence should be addressed. E-mail: dab87@cornell.edu

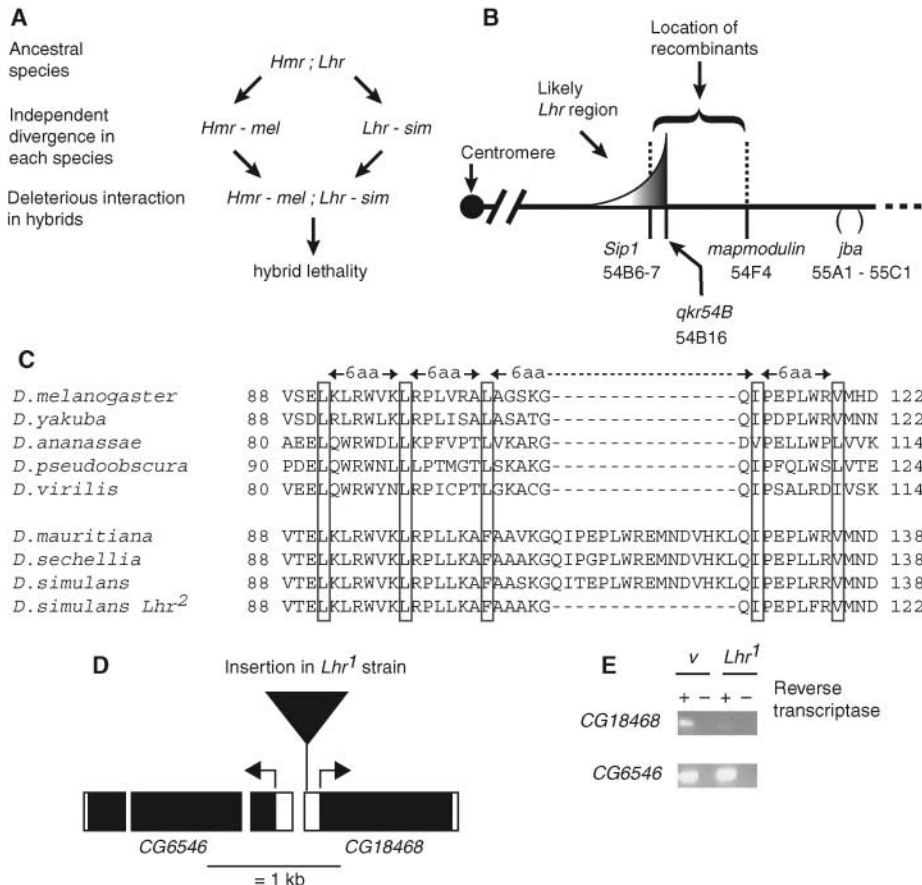


Fig. 1. CG18468 encodes *Lhr*. (A) Model of *Hmr* and *Lhr* functional divergence and the interaction that causes hybrid lethality. Lethality results from the interaction between the *D. melanogaster Hmr* allele (*Hmr-mel*) and the *D. simulans Lhr* allele (*Lhr-sim*). (B) Map of *Lhr* region in *D. simulans*. Genetic markers and estimated cytological locations in *D. melanogaster* are shown below the line. Ten recombinants between *jba* and *Lhr* were selected and cross-overs mapped within a region of approximately 480 kb; the most proximal recombinant was between *Sip1* and *qkr54B* (diagram not to scale). (C) *CG18468* has a characteristic leucine zipper-like structure in all *Drosophila* species except *D. simulans*, *D. mauritiana*, and *D. sechellia*, which have a 16-amino acid insertion; this insertion is lacking in the *D. simulans* rescue strain *Lhr²*. (D) Map of *CG18468* region at 54B7 and insertion in the *Lhr¹* strain. Black boxes, coding regions; unfilled boxes, UTRs; arrows, predicted translation start sites. The large triangle represents an insertion of ~4 kb (triangle not to scale) located between nucleotides 11 and 13 of the predicted *CG18468* mRNA in *Lhr¹*. (E) The insertion in *Lhr¹* reduces the level of mRNA of *CG18468* but not of *CG6546*. RT-PCR with larval RNA from a *vermillion* (*v*)-marked *D. simulans* strain and from the *Lhr¹* strain.

The *D. simulans* mutation *Lhr¹* suppresses the lethality of these F1 hybrid males (13). A mutant allele of the X-linked *D. melanogaster* gene *Hmr* similarly suppresses hybrid male lethality (14). *Hmr* encodes a rapidly evolving protein with sequence similarity to the myb/SANT-like domain in Adf-1 (MADF) class of DNA binding proteins (14). Genetic interaction studies (15, 16) suggested that *Hmr* and *Lhr* interact to cause lethality in a manner consistent with the Dobzhansky-Muller model (Fig. 1A).

Lhr¹ maps 1.7 centimorgans from the visible marker *jba* on chromosome 2R (17). We identified recombinants between *Lhr¹* and *jba* and typed them using molecular markers that distinguish the *Lhr¹* and *jba D. simulans* strains (Fig. 1B). On the basis of the distribution of recombinants, *Lhr¹* is likely within several hundred kilobases centromere-proximal to *qkr54B*.

Because of the paucity of visible markers in *D. simulans*, we did not attempt to obtain a proximal limit for *Lhr* by mapping. Instead, we searched preliminary assemblies of the *D. simulans* genome for candidate genes on the basis of similarities to *Hmr*, namely higher-than-average divergence between *D. melanogaster* and *D. simulans* and a possible role in DNA or chromatin binding. Among ~37 genes, we first examined *CG18468* because it contains a boundary element-associated factor 32/Su(var)3-7/ Stonewall (BESS) domain. The BESS domain is found in 21 *Drosophila* proteins, often associated with MADF domains, and mediates protein-protein interactions (18). *Hmr* is predicted to encode a protein with two MADF domains (14), and we detected a putative BESS domain (fig. S1), suggesting a possible functional relationship between *CG18468* and *Hmr*.

Most predicted *D. simulans* proteins are >90% identical to their *D. melanogaster* orthologs. In contrast, *CG18468* has only ~80% identity, caused by amino acid divergence and by a 16-amino acid insertion in *D. simulans* (Fig. 1C and fig. S2). The estimated average divergence of *CG18468* is similar to *Hmr* (14), measuring 0.078 at nonsynonymous sites (*K_A*) and 0.106 at synonymous sites (*K_S*). This *K_A* value, but not the *K_S* value, is substantially higher than the average value between *D. melanogaster* and *D. simulans* (19). Again similar to *Hmr*, *CG18468* is highly diverged outside the *melanogaster* subgroup (fig. S2), and both genes apparently lack orthologs outside of *Drosophila*.

We discovered that *CG18468* is mutated in the *Lhr¹* rescue strain, which contains an insertion of ~4 kb in the predicted 5' untranslated region (UTR) (Fig. 1D) that appears to be a moderately repetitive retrotransposed sequence. This insertion is not found in any of the five strains from which genome sequence is available nor from 11 additional lines we sequenced (19). *CG18468* is adjacent to and divergently transcribed from *CG6546* (Fig. 1D), so the insertion in the *Lhr¹* rescue strain could potentially affect the transcription of either or both of these

genes. Reverse transcription polymerase chain reaction (RT-PCR) products, derived from RNA from the critical early larval stage (15), showed that both genes are transcribed in a control strain but that *CG18468* transcription is strongly reduced in the *Lhr¹* rescue strain (Fig. 1E). These data suggest that the *Lhr¹* phenotype is caused by reduced expression of *CG18468*.

We cloned the wild-type *CG18468* gene from *D. simulans* and transformed *D. melanogaster* with *P* element vectors containing a *D. simulans CG18468* cDNA under the control of *Saccharomyces cerevisiae* Upstream Activity Sequences (*UAS*), henceforth referred to as *UAS-Dsim/Lhr*. Expression was induced from a second, independently segregating transgene expressing the *S. cerevisiae* transcriptional activator *GAL4* (Fig. 2). Control crosses using two different *GAL4*-expressing transgenes suggested that activation of *UAS-Dsim/Lhr* does not cause lethality in *D. melanogaster*, as evidenced by the similar numbers of progeny inheriting the *GAL4* driver ("red eyed" in Table 1) compared to those that did not ("orange eyed" and "white eyed") (Table 1 and table S1).

This result demonstrated that we could introduce both *UAS-Dsim/Lhr* and the *GAL4*-

expressing transgenes into hybrids from the *D. melanogaster* parent (Fig. 2). In contrast to the intraspecific control cross, when the same *D. melanogaster* females were crossed to *D. simulans Lhr¹* males, only half of the expected hybrid males carrying the *GAL4*-expressing transgene were obtained (Table 1). PCR-based genotyping confirmed our inference that *Lhr¹*-rescued males carrying only the *GAL4*-expressing transgene are viable, whereas those carrying both transgenes and thus expressing *UAS-Dsim/Lhr* are lethal (table S1). The reduced viability in some crosses of *Lhr¹*-rescued males containing only the *UAS-Dsim/Lhr* transgene is likely due to maternal inheritance of the *GAL4* protein (table S1).

These results suggest that expression of *UAS-Dsim/Lhr* complements the *Lhr¹* hybrid rescue phenotype. We confirmed that *UAS-Dsim/Lhr* expression is not generally lethal to hybrids compared with *D. melanogaster* pure species by testing for effects in hybrid males rescued by a mutation in *Hmr*. We found that both *D. melanogaster* control males and male hybrids rescued by the null mutation *Df(1)Hmr⁻* are fully viable when expressing *UAS-Dsim/Lhr* (Table 1). RT-PCR experiments demonstrated that *UAS-Dsim/Lhr* was expressed in these crosses (fig. S3).

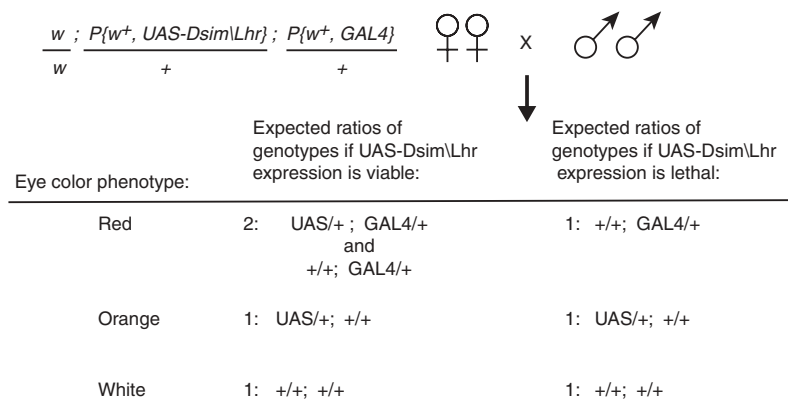


Fig. 2. Complementation crosses to test for suppression of hybrid male rescue. Female parents are heterozygous for both transgenes, each marked with *w⁺* producing intermediate levels of eye pigmentation. The *GAL4*-containing transformants have darker eye colors and are epistatic to the lighter-colored *UAS*-containing transformants. The red-eyed class is therefore potentially composed of two distinct genotypes.

Table 1. Number of offspring recovered from complementation tests of hybrid rescue mutations by *UAS-Dsim/Lhr* expression. Full parental genotypes and female progeny are shown in table S1, crosses 9 to 12. *UAS* indicates *D. simulans Lhr* under yeast *UAS* transcriptional control; *GAL4* indicates yeast *GAL4* protein driven by the *Actin5C* promoter. In the absence of viability effects, the ratio of red-eyed:orange-eyed:white-eyed males will be 2:1:1. Deviations from this ratio were tested by χ^2 tests. Results for the control cross and the cross with *Df(1)Hmr⁻* were not significantly different from this ratio ($P > 0.05$). Results for the crosses with *Lhr¹* and *Hmr¹* were significantly different from this ratio ($P < 0.001$).

| Progeny | | <i>D. melanogaster</i> control | <i>Lhr¹</i> | <i>Df(1)Hmr⁻</i> | <i>Hmr¹</i> |
|------------------|-----------------------------|--------------------------------|------------------------|-----------------------------|------------------------|
| Phenotype | Genotype | | | | |
| Red-eyed male | UAS/+;GAL4/+ and +/+;GAL4/+ | 485 | 89 | 169 | 22 |
| Orange-eyed male | UAS/+;+/+ | 214 | 9 | 82 | 7 |
| White-eyed male | +/+;+/+ | 262 | 94 | 95 | 33 |

We concluded that *UAS-Dsim/Lhr* expression specifically complements the *Lhr^l* mutation in hybrids, that *CG18468* is *Lhr*, and that *Lhr* is a major-effect hybrid lethality gene.

For *Lhr* to fit the Dobzhansky-Muller model of functional divergence, *D. simulans Lhr*, but not *D. melanogaster Lhr*, must cause hybrid lethality (Fig. 1A). Crosses with three different *D. melanogaster Lhr⁻* deletions produced essentially only F1 hybrid females, demonstrating that removal of *D. melanogaster Lhr* does not suppress F1 male lethality (fig. S4 and table S2).

Genetic and molecular analyses have demonstrated that *Hmr^l* retains partial *Hmr* activity (14, 15). In contrast to the results shown in Table 1, which used the null allele *Df(1)Hmr⁻*, we found that rescue of hybrids by the hypomorphic mutation *Hmr^l* is suppressed by *D. simulans Lhr* expression (Table 1 and table S1). These data suggest that the lethal effect of *D. simulans Lhr* requires the presence of *D. melanogaster Hmr* function. The deleterious effects of a *D. melanogaster Hmr⁺* duplication are suppressed by *Lhr^l* (15, 16), results that suggest, based on our characterization of the *Lhr^l* mutation, that *D. melanogaster Hmr* requires a functional *D. simulans Lhr* to cause lethality. These reciprocal genetic interactions are consistent with the model of *Hmr* and *Lhr* forming a Dobzhansky-Muller pair of interacting genes (Fig. 1A).

Functional divergence between species led us to examine the evolutionary forces driving the sequence divergence of *Lhr*. The high K_A/K_S value of 0.731 between *D. melanogaster* and *D. simulans* is consistent with either positive selection or relaxed selective constraint. We sequenced multiple alleles of *Lhr* from *D. melanogaster* and *D. simulans* and performed a McDonald-Kreitman test (19). The results of this test rejected the null hypothesis that these

genes are evolving neutrally (Fisher's Exact Test, $P = 0.011$) and suggested that there is an excess of nonsynonymous fixations between the species (table S3). Phylogenetic analyses further suggest that the K_A/K_S ratio has increased on branches leading to *D. melanogaster* and its sibling species (fig. S5).

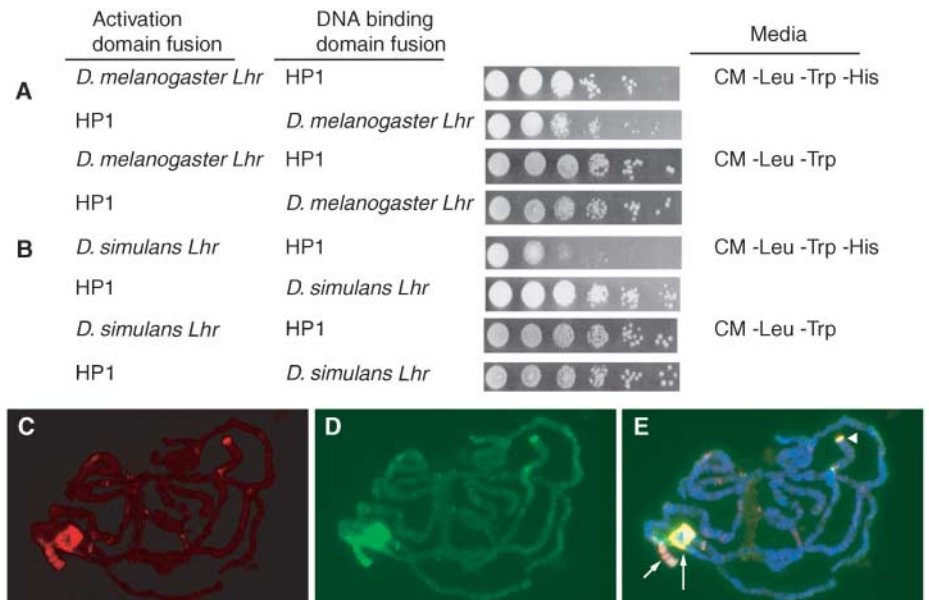
The McDonald-Kreitman and K_A/K_S tests only consider alignable regions of the *Lhr* coding region. *Lhr* from *D. simulans* and its sister species *D. mauritiana* and *D. sechellia* each contain a 16–amino acid insertion, interrupting a potential leucine zipper domain, relative to *D. melanogaster* and outgroup species (Fig. 1C and fig. S2). Notably, we found that this insertion is precisely deleted in a second *D. simulans* stock named *Lhr²*, which also produces viable F1 hybrid males (20). Although *Lhr²* contains additional amino acid substitutions relative to *Lhr⁺* alleles, its hybrid rescue phenotype suggests that the functional divergence of *D. simulans Lhr* may be caused by the 16–amino acid insertion.

Heterochromatin Protein 1 (HP1) is a chromodomain-containing protein that localizes to heterochromatic regions of chromosomes and is required to maintain heterochromatic states (21). LHR was previously identified (as CG18468) as interacting with HP1 in a yeast two-hybrid assay (22). We confirmed this interaction (Fig. 3A), and discovered that *D. simulans* LHR also interacts with *D. melanogaster* HP1 (Fig. 3B). Because *D. simulans* HP1 is nearly identical to *D. melanogaster* HP1 (fig. S6) we hypothesize that *D. simulans* LHR also binds to *D. simulans* HP1. This apparent conservation of HP1-binding function of LHR suggests that the intraspecific function of *Lhr* is conserved between *D. melanogaster* and *D. simulans*, in contrast to the interspecific function for hybrid lethality, which we have shown is specific only to *D. simulans Lhr*.

A. D. melanogaster LHR–yellow fluorescent protein (YFP) fusion protein accumulated in a small number of foci (usually 1 to 2) in salivary gland nuclei (fig. S7), similar to HP1 (23). In polytene chromosomes, HP1 accumulates predominantly in the chromocenter and along the highly heterochromatic fourth chromosome as well as at telomeres and a number of bands along the euchromatic arms (24). LHR–YFP has a similar pattern and predominantly colocalizes with HP1 (Fig. 3, C to E). We suggest that *Lhr* may be coevolving with rapidly evolving heterochromatic repetitive DNAs, consistent with the hypothesis that the molecular drive inherent in repetitive DNAs contributes to hybrid incompatibilities and speciation (25, 26).

Hmr and *Lhr* cause F1 hybrid lethality because they are partially or fully dominant. The large number of HI genes estimated from other studies (27) may be mechanistically distinct because they are recessive and only cause HI when homozygous in F2 hybrids or in interspecific introgressions. However, our results also show that the interaction of *Hmr* and *Lhr* alone is insufficient to recapitulate hybrid lethality, because control crosses showed that expression of *D. simulans Lhr* does not cause lethality in a *D. melanogaster* pure-species background (Table 1 and table S1). Pontecorvo suggested that an interaction among the *D. melanogaster X* (which contains *Hmr*), *D. simulans* chromosome II (which contains *Lhr*), and *D. simulans* chromosome III causes hybrid lethality (28). Hybrid lethality may therefore be enhanced by a multilocus interaction involving additional genes. Alternatively, *Hmr* and *Lhr* may be the only major-effect genes, but their lethal interaction requires a hybrid genetic background. We suggest that altered chromosome morphology and chromatin structure in hybrids due to the

Fig. 3. LHR interacts and colocalizes with HP1. (A) *D. melanogaster* LHR interacts with *D. melanogaster* HP1. Yeast two-hybrid interactions were detected by activation of *HIS3* and growth on media lacking histidine; loading controls [complete media (CM) -Leu -Trp] contain histidine. (B) *D. simulans* LHR interacts with *D. melanogaster* HP1. (C to E) Colocalization of *D. melanogaster* YFP::LHR and HP1 on salivary gland polytene chromosomes. Chromosomes from *P{UAS-YFP::Lhr}168-3/+;P{GawB}C147/+* third-instar larvae were incubated with primary antibodies to GFP and HP1, which were detected using rhodamine red-X-conjugated (red) and cyanine-conjugated (green) secondary antibodies, respectively. (C) Antibody to GFP to detect YFP::LHR. (D) Antibody to HP1. (E) Merge with 4',6'-diamidino-2-phenylindole signal (blue) to detect DNA. A predominant colocalization occurs at the chromocenter (long arrow), fourth chromosome (short arrow), and a telomere (arrowhead).



cumulative effects of species-specific differences in satellites, transposable elements, and other repetitive DNAs cause this hybrid genetic background effect.

References and Notes

- J. A. Coyne, H. A. Orr, *Speciation* (Sinauer, Sunderland, MA, 2004).
- C.-T. Ting, S.-C. Tsaur, M.-L. Wu, C.-I. Wu, *Science* **282**, 1501 (1998).
- D. A. Barbash, P. Awadalla, A. M. Tarone, *PLoS Biol.* **2**, e142 (2004).
- D. C. Presgraves, L. Balagopal, S. M. Abmayr, H. A. Orr, *Nature* **423**, 715 (2003).
- J. B. Hutchinson, *J. Genet.* **25**, 281 (1932).
- P. Christie, M. R. MacNair, *J. Hered.* **75**, 510 (1984).
- A. R. Carvajal, M. R. Gandarela, H. F. Naveira, *Genetica* **98**, 1 (1996).
- S. Kazianis *et al.*, *Genes Chromosomes Cancer* **22**, 210 (1998).
- A. L. Sweigart, L. Fishman, J. H. Willis, *Genetics* **172**, 2465 (2006); published online 16 January 2006.
- E. L. Cabot, A. W. Davis, N. A. Johnson, C.-I. Wu, *Genetics* **137**, 175 (1994).
- X. R. Maside, J. P. Barral, H. F. Naveira, *Genetics* **150**, 745 (1998).
- Y. Tao, Z.-B. Zeng, J. Li, D. L. Hartl, C. C. Laurie, *Genetics* **164**, 1399 (2003).
- T. K. Watanabe, *Jpn. J. Genet.* **54**, 325 (1979).
- D. A. Barbash, D. F. Siino, A. M. Tarone, J. Roote, *Proc. Natl. Acad. Sci. U.S.A.* **100**, 5302 (2003).
- D. A. Barbash, J. Roote, M. Ashburner, *Genetics* **154**, 1747 (2000).
- H. A. Orr, S. Irving, *Genetics* **155**, 225 (2000).
- M.-T. Yamamoto, M. Kamo, S. Yamamoto, T. K. Watanabe, *Genes Genet. Syst.* **72**, 297 (1997).
- V. Bhaskar, A. J. Courey, *Gene* **299**, 173 (2002).
- Materials and methods are provided as supporting material on *Science* Online.
- H. A. Orr, personal communication.
- J. C. Eissenberg, S. C. Elgin, *Curr. Opin. Genet. Dev.* **10**, 204 (2000).
- L. Giot *et al.*, *Science* **302**, 1727 (2003).
- J. A. Powers, J. C. Eissenberg, *J. Cell Biol.* **120**, 291 (1993).
- L. Fanti, M. Berloco, L. Piacentini, S. Pimpinelli, *Genetica* **117**, 135 (2003).
- G. Dover, *Nature* **299**, 111 (1982).
- S. Henikoff, K. Ahmad, H. S. Malik, *Science* **293**, 1098 (2001).
- J. Mallet, *Trends Ecol. Evol.* **21**, 386 (2006).
- G. Pontecorvo, *J. Genet.* **45**, 51 (1943).
- We thank the *Drosophila* Genomics Resource Center for cloning vectors; H. A. Orr, M.-T. Yamamoto, and the Bloomington *Drosophila* Stock Center for fly stocks; C. Langley, I. Liachko, T. Schlenke, and J. Werner for helpful discussions; and E. Alani, C. Aquadro, A. Clark, and B. Lazzaro for comments on the manuscript. Supported by NIH grant R01 GM074737-01. Accession numbers mentioned in the manuscript have been deposited in GenBank under the numbers EF044038-62, EF057388-9, and BK005905-14.

Supporting Online Material

www.sciencemag.org/cgi/content/full/314/5803/1292/DC1

Materials and Methods

Figs. S1 to S7

Tables S1 to S3

References

16 August 2006; accepted 20 October 2006

10.1126/science.1133953

Localization of Iron in *Arabidopsis* Seed Requires the Vacuolar Membrane Transporter VIT1

Sun A. Kim,^{1*} Tracy Punshon,^{1*} Antonio Lanzirrotti,² Liangtao Li,³ José M. Alonso,⁴ Joseph R. Ecker,⁵ Jerry Kaplan,³ Mary Lou Guerinot^{1†}

Iron deficiency is a major human nutritional problem wherever plant-based diets are common. Using synchrotron x-ray fluorescence microtomography to directly visualize iron in *Arabidopsis* seeds, we show that iron is localized primarily to the provascular strands of the embryo. This localization is completely abolished when the vacuolar iron uptake transporter VIT1 is disrupted. Vacuolar iron storage is also critical for seedling development because *vit1-1* seedlings grow poorly when iron is limiting. We have uncovered a fundamental aspect of seed biology that will ultimately aid the development of nutrient-rich seed, benefiting both human health and agricultural productivity.

Iron is the most important yet problematic of the essential elements required by plants. It is needed for life-sustaining processes from photosynthesis to respiration, yet it can be toxic at high levels due to its propensity to form hydroxyl radicals that can damage cellular constituents. Like animal cells, plant cells can safely store iron in ferritin (*I*). However, unlike animal cells, plant cells also have vacuoles in which iron and other potentially toxic metals can be sequestered. Most efforts to date at increasing the iron content of staple foods have been

focused on increasing seed ferritin levels (2–4), but the contribution of the vacuole to seed iron storage has remained largely unexplored.

In yeast, the vacuole serves as the main intracellular storage compartment for iron (5–7). The yeast *CCC1* (Ca²⁺-sensitive cross-complement 1) gene encodes an iron/manganese transporter that mediates the accumulation of these metals in the vacuole (8). We have characterized the *Arabidopsis* ortholog of yeast *CCC1*, VIT1 (vacuolar iron transporter 1; At2g01770), in order to address the role of the vacuole in iron homeostasis. VIT1 shows 62% amino acid similarity to the yeast *CCC1* protein, and secondary-structure analysis programs predict five possible transmembrane domains, consistent with the model previously proposed for yeast *CCC1*. VIT1-like proteins can be found throughout the plant kingdom, with a distinct clustering of dicot and monocot VIT1-like sequences (Fig. 1A).

To determine if VIT1 is a true ortholog of *CCC1*, we expressed *VIT1* in *ccc1* mutant yeast that are sensitive to high amounts of extra-

cellular iron and thus fail to grow on media containing elevated levels of iron. This sensitivity is due to the inability of the *ccc1* mutant to store iron in the vacuole, leading to increased accumulation of cytosolic iron (8). Expression of *VIT1* sustained the growth of the *ccc1* mutant yeast on high-iron medium (Fig. 1B). When VIT1 was expressed in *ccc1* mutant yeast, vacuolar iron was increased threefold compared to control cells (Fig. 1C). Vacuolar manganese was also increased in yeast cells expressing *VIT1* (Fig. 1D). The increases seen are similar to those conferred by expression of the *CCC1* gene (6). No increases were seen in Zn or Cd. We also examined the effect of *VIT1* expression on iron uptake. Overexpression of *CCC1* in yeast cells decreases cytosolic iron levels, leading to increased expression of high-affinity iron transporters in the plasma membrane (9). The iron uptake rate of yeast cells overexpressing *VIT1* was markedly increased relative to *ccc1* cells (Fig. 1E). This result, together with the increased metal content of the vacuole, provides functional proof that VIT1 mediates iron sequestration into vacuoles.

We next investigated the localization of VIT1 using a green fluorescent protein (GFP)-tagged version of the VIT1 protein. The GFP-VIT1 fusion protein complements the *ccc1* mutant phenotype (fig. S1), indicating that GFP tagging does not disrupt the biochemical function or the localization of VIT1. In yeast, GFP-VIT1 colocalizes to the vacuolar membrane with the FM4-64 marker (fig. S1). In transgenic *Arabidopsis* plants that stably express a *GFP-VIT1* gene driven by the 35S promoter, the GFP fluorescence is localized to the vacuolar membrane (Fig. 2, A to D). In Fig. 2, A and C, the VIT1-GFP staining is only seen on the side of the nucleus facing the interior of the cell, that is, distinguishing it from staining of the plasma membrane, which would follow the cell periphery.

¹Department of Biological Sciences, Dartmouth College, Hanover, NH 03755, USA. ²Consortium for Advanced Radiation Sources, University of Chicago, Chicago, IL 60637, USA. ³Department of Pathology, University of Utah School of Medicine, Salt Lake City, UT 84132, USA. ⁴Department of Genetics, North Carolina State University, Raleigh, NC 27695, USA. ⁵Plant Biology and Genomic Analysis Laboratories, The Salk Institute for Biological Studies, La Jolla, CA 92037, USA.

*These authors contributed equally to this work.

†To whom correspondence should be addressed. E-mail: guerinot@dartmouth.edu